



# Selective determination of L-dopa in the presence of uric acid and ascorbic acid at a gold nanoparticle self-assembled carbon nanotube-modified pyrolytic graphite electrode

Guangzhi Hu<sup>a,c</sup>, Long Chen<sup>b</sup>, Yong Guo<sup>a</sup>, Xiaolai Wang<sup>b,\*</sup>, Shijun Shao<sup>a,\*</sup>

<sup>a</sup> Key Laboratory for Natural Medicine of Gansu Province, Lanzhou Institute of Chemical Physics, Chinese Academy of Sciences, Lanzhou 730000, PR China

<sup>b</sup> State Key Laboratory for Oxo Synthesis and Selective Oxidation, Lanzhou Institute of Chemical Physics, Chinese Academy of Sciences, Lanzhou 730000, PR China

<sup>c</sup> Graduate School of the Chinese Academy of Sciences, Beijing 100039, PR China

## ARTICLE INFO

### Article history:

Received 4 March 2010

Accepted 24 March 2010

Available online 31 March 2010

### Keywords:

Gold nanoparticles

Carbon nanotubes

Self-assembly

L-dopa

Pyrolytic graphite electrode

## ABSTRACT

Gold nanoparticle-functionalized carbon nanotubes (AuNP-CNT) have been prepared by a novel self-assembly method. The new material has been characterized by transmission electron microscopy (TEM) and X-ray diffraction (XRD) and utilized for constructing AuNP-CNT-modified pyrolytic graphite electrode (AuNP-CNT/PGE) to investigate the electrochemical behavior of L-dopa in neutral phosphate buffer solution. Compared to bare PG electrode, AuNP-CNT/PGE shows novel properties towards the electrochemical redox of L-dopa in phosphate buffer solution at pH 7.0. The oxidation potential of L-dopa shows a significant decrease at the AuNP-CNT/PGE. The oxidation current of L-dopa is about 5-fold higher than that of the unmodified PGE. Using differential pulse voltammetry (DPV) method, the oxidation current is well linear with L-dopa concentration in the range of 0.1–150  $\mu$ M, with a detection limit of about 50 nM ( $S/N = 3$ ). The proposed electrode can also effectively avoid the interference of ascorbic acid and uric acid, making the proposed sensor suitable for the accurate determination of L-dopa in both pharmaceutical preparations and human body fluids.

© 2010 Elsevier Ltd. All rights reserved.

## 1. Introduction

Parkinson's disease is a chronic, progressive neurodegenerative movement disorder that occurs when the substantia nigra of the mid-brain dies and fails to produce enough dopamine [1]. This condition causes tremors, rigidity, poor balance, and dyskinesia. Because it cannot penetrate the blood–brain barrier, dopamine cannot be effectively used for the treatment of this serious disease [2]. L-dopa (levodopa, 3,4-dihydroxy-L-phenylalanine) is widely used as a source of dopamine in the treatment of most patients with Parkinson's disease and epilepsy [3]. This drug can be principally metabolized by an enzymatic reaction (dopa-decarboxylase) to dopamine compensating for the deficiency of dopamine in the brain. With its serious side effects with long-term use on human health, e.g. gastritis, paranoia, and dyskinesia [4,5], L-dopa should be given an accurate analysis in both pharmaceutical formulations and biological fluids. At present, several technologies have been reported for L-dopa analysis, such as titration [6], spectrophotometry [7], and high-performance liquid chromatography [8]. These determination methods often require some complicated and time-consuming pretreatments and/or experimental equipments.

As catecholamine compounds can be oxidized with electrochemical technology [9], herein, L-dopa can also be detected with electrochemical method. Unfortunately, most unmodified solid electrodes show a slow electron transfer for the electrochemical oxidation of L-dopa with a high overpotential. The oxidation product of L-dopa easily adsorbs at the bare electrode surface, leading to the poor reproducibility and repeatability of these unmodified electrodes. Furthermore, some small biomolecules, e.g. uric acid (UA) and ascorbic acid (AA), have similar oxidation potential as that of L-dopa and show serious interference for the determination of L-dopa [10]. To overcome these problems, many chemically modified electrodes have been reported for the L-dopa determination. Teixeira et al. fabricated a carbon paste electrode modified with trinuclear ruthenium ammine complex (Ru-red) supported on Y-type zeolite for the voltammetric determination in a acetate buffer at pH 4.8, with a detection limit of about 85  $\mu$ M [11]. Bergamini et al. applied a gold screen-printing electrode to the monitor of L-dopa in stationary solution and a flow system at pH 3.0 [12]. Sivanesan and John fabricated a glassy carbon electrode modified with tetraaminophthalocyanatonickel (II) film for the selective determination of L-dopa in the presence of ascorbic acid [13].

Nanoscale materials have attracted considerable attention of the analysts in the last decade due to their special physical and chemical properties [14–18]. Goyal group developed a number of nanomaterial-modified electrode and applied them to the

\* Corresponding author. Fax: +86 931 8277088.

E-mail addresses: [xlwang@lzb.ac.cn](mailto:xlwang@lzb.ac.cn) (X. Wang), [shaoguo@licp.cas.cn](mailto:shaoguo@licp.cas.cn) (S. Shao).

electrochemical determination of biomolecules and drugs, e.g. dexamethasone [19], triamcinolone [20], 2',3'-dideoxyadenosine [21], adenosine and guanosine [22], paracetamol [23], uric acid [24], dopamine [25] and inosine [26]. Yan et al. proved that single-wall carbon nanotubes can effectively decrease the oxidation potential of L-dopa and can be utilized to prepare a single-wall carbon nanotube-modified glassy carbon electrode for the determination of L-dopa, with a detection limit of about  $0.3 \mu\text{M}$  [27]. Xiang et al. reported a multi-wall carbon nanotubes-Nafion modified glassy carbon electrode for the adsorption stripping voltammetry of L-dopa, with a detection limit of about  $50 \text{ nM}$  [28]. Mathiyarasu and Nyholm constructed a poly-(3,4-ethylenedioxythiophene)-single-walled carbon nanotube composite-modified microelectrode and applied it to the electrochemical determination of L-dopa, with a detection limit of  $0.1 \mu\text{M}$  [29]. Shahrokhian and Asadian reported a glassy carbon electrode modified by a bilayer of multi-walled carbon nanotube and poly-pyrrole doped with tiron for the electrochemical determination of L-dopa in the presence of AA, with a detection limit of  $0.1 \mu\text{M}$  [30].

It is a fact that gold nanoparticles show good electrocatalytic activity towards the electrochemical oxidation of dopamine [31–33]. In this paper, we have synthesized gold nanoparticle-functionalized multi-wall carbon nanotubes by a self-assembly

method. The new material was applied to investigate the electrochemical behavior of L-dopa in neutral phosphate buffer solution (PBS). Experimental data show that the proposed electrode can effectively decrease the oxidation potential of L-dopa. Using the differential pulse voltammetry for the accurate determination of L-dopa, the oxidation current is proportional with its concentration in the range of  $0.1\text{--}150 \mu\text{M}$ , with a detection limit about  $50 \text{ nM}$ . Meanwhile, the proposed sensor can also effectively avoid the interference of AA and UA and has been successfully applied to the determination of L-dopa formulations with high sensitivity and good selectivity.

## 2. Experimental

### 2.1. Chemicals

Chloroauric acid and L-dopa hydrochloride were purchased from the Sinopharm Chemical Reagent Co. (Shanghai, China). Benzyl Mercaptan (BM), uric acid and ascorbic acid were purchased from Alfa-Aesar (Tianjin, China). L-dopa capsules were purchased from the Shanghai Roche Pharmaceuticals (Shanghai, China). All other chemicals are of analytical grade and used as received.

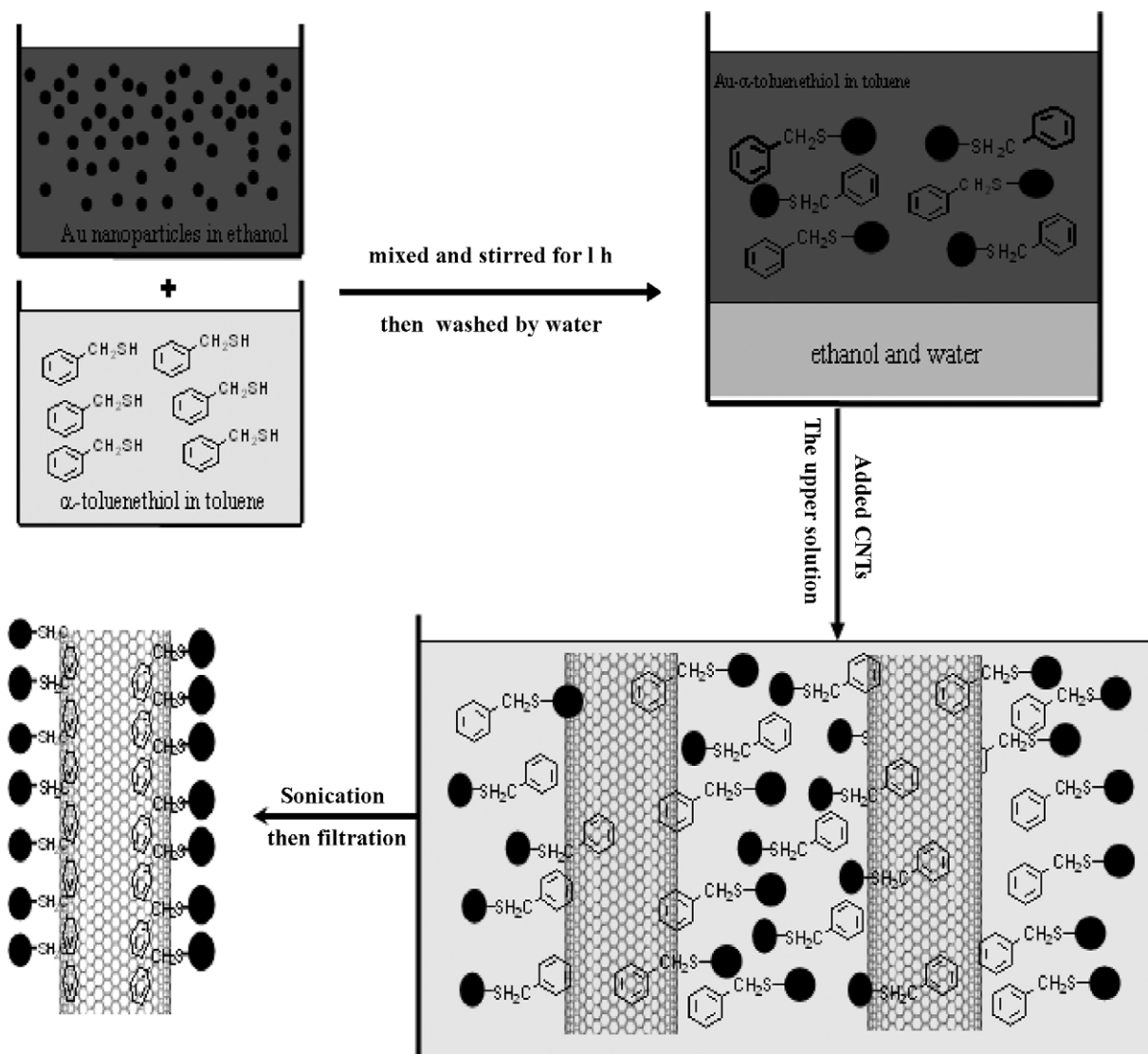


Fig. 1. Preparation scheme of AuNP-CNTs.

## 2.2. Synthesis of AuNP-CNTs

High-quality multi-wall carbon nanotubes were synthesized by chemical vapor deposition method using Co/La<sub>2</sub>O<sub>3</sub> as catalyst and ethylene as carbon source in a tubular quartz reactor. The detailed experimental procedure is given in our previous report [34]. Gold nanoparticles were synthesized according to the former literature [35]. The synthesis procedure of gold nanoparticles self-assembled CNTs, illustrated as in Fig. 1, was similar to our previous report [36]. Briefly, the obtained Au colloidal solution was added into a toluene solution containing Benzyl Mercaptan (BM) and given a stirring for 1 h, and then equal volume of distilled water was added to the solution. A liquid in two phases was obtained. The upper dark brown solution was BM-modified Au/toluene solution and was washed with distilled water to remove the ethanol completely. About 33 mg of multi-walled CNTs was added to a certain volume of toluene and given an ultrasonication for about 2 h to form a CNTs/toluene suspension. The as-prepared suspension was mixed with the above-mentioned BM-modified Au/toluene solution and ultrasonicated for 12 h until all Au nanoparticles were anchored on CNTs. The AuNP-CNT was separated from the mixture via suction filtration and then washed by ethanol completely.

## 2.3. Preparation of AuNP-CNTs/PGE

Bare PGE (2 mm in diameter, Tianjin Aidahengsheng Co., China) was carefully polished with 1.0, 0.3, and 0.05 μm alumina powders in series, and then treated with 50% nitric acid, ethanol and water in

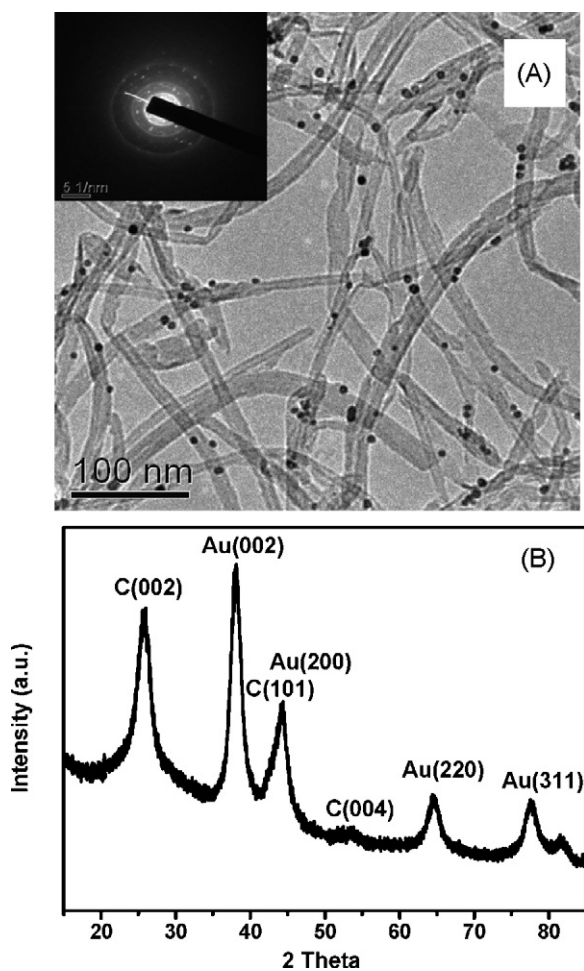


Fig. 2. TEM image (A) and XRD pattern (B) of Au-CNTs. (A, inset): SAED image of Au-CNTs.

an ultrasonic bath, respectively. 10 mg of AuNP-CNTs were added to 10 mL of *N,N*-dimethylformamide (DMF) under ultrasonic agitation to give a black suspension. The AuNP-CNT/PGE was prepared by casting 10 μL of AuNP-CNT suspension on the pretreated PGE surface and dried under an infrared lamp.

## 2.4. Measurements

The morphology of the Au-CNT nanocomposite was determined with a JEOL 2010 TEM (JEOL, Japan) equipped with a LaB6 filament at 200 kV and an energy dispersive X-ray analyzer (EDAX, USA). XRD data was obtained by an X'Pert PRO Multi-purpose Diffractometer (PANalytical, Netherlands) using Cu Kα radiation ( $k=0.15418$  nm).

Voltammetric measurements were carried out on a CHI660C electrochemical workstation (CHI Instrument, Shanghai). All measurements were performed in a conventional three-electrode cell, consisting of an unmodified PGE (Tianjin Aidahengsheng Technology Co., China) or the AuNP-CNT-modified PGE working electrode, a saturated calomel electrode (SCE) reference and a platinum wire counter electrode. 0.1 M phosphate buffer solution at pH 6.9 was prepared from KH<sub>2</sub>PO<sub>4</sub> and K<sub>2</sub>HPO<sub>4</sub> and its pH was adjusted value with 1 M H<sub>2</sub>SO<sub>4</sub> or NaOH solution. Prior to each electrochemical measurement, the electrolyte solution was deoxygenated by bubbling with high-pure nitrogen for 30 min.

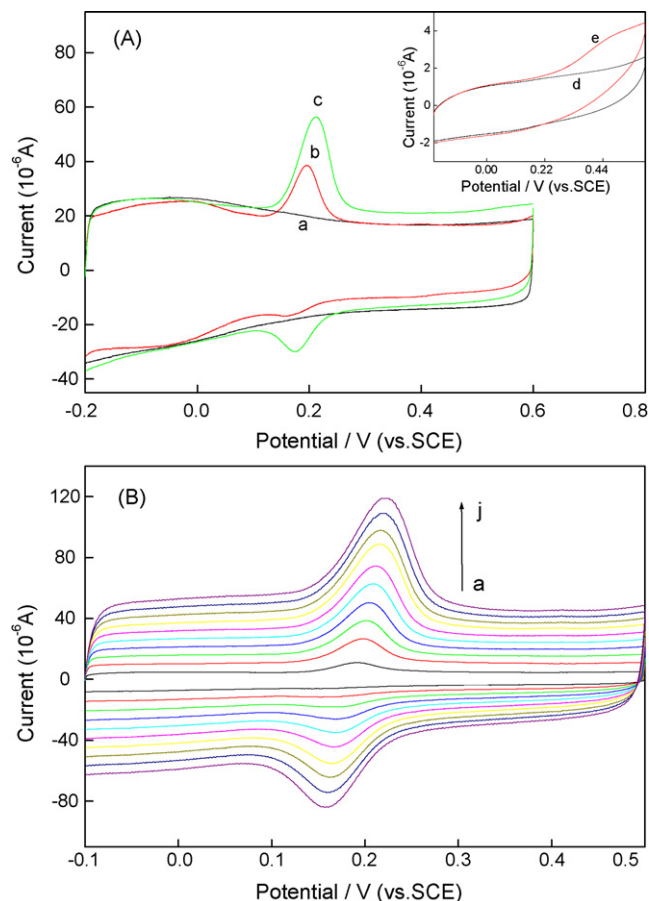


Fig. 3. (A) Cyclic voltammograms of AuNP-CNT/PGE (curve a and c) and CNT/PGE (curve b) in the absence (curve a) and presence (curve b and c) of 20 μM L-dopa in 0.1 M PBS at pH 7.0, inset is CV curves of bare PGE in 0.1 M PBS at pH 7.0 without (curve d) and with (curve e) 20 μM L-dopa; (B) cyclic voltammograms of AuNP-CNT/PGE in 0.1 M PBS (pH 7.0) containing 20 μM L-dopa at different scanning rate: a → j, 20, 40, 60, 80, 100, 120, 140, 160, 180, and 200 mV/s.

### 3. Results and discussion

#### 3.1. Characterization of AuNP-CNTs

Fig. 2A presents a typical TEM image of the as-prepared AuNP-CNTs. The spherical gold nanoparticles are homogeneously dispersed on CNTs without significant aggregation and the diameter of them is from 5 to 10 nm. No dissociated Au nanoparticle is observed on the background of TEM image, indicating that these Au nanoparticles are strongly adhered on the CNT surface. The selected area electron diffraction (SAED) pattern in Fig. 1 (inset) shows that these Au nanoparticles on CNT surface are polycrystalline structure. XRD pattern of AuNP-CNTs shows (002), (101) and (004) reflections of graphite, as well as (002), (200), (220) and (311) reflections of gold, indicating that metallic Au phase exists in the as-prepared nanoscale hybrid. According to the Scherrer equation [37], the average diameter of the gold nanoparticles was calculated about 9.5 nm, consistent with previous TEM results.

#### 3.2. Electrochemical behavior of L-dopa

The electrochemical behavior of L-dopa was investigated with cyclic voltammetry (CV) in 0.1 M phosphate buffer solution at pH 6.9. As shown in Fig. 3A (inset), a weak response and low electron transaction for L-dopa is observed on a bare PGE. A broad oxidation peak of L-dopa is at 0.486 V, with a broad potential region from 0.2 to 0.6 V. The CNT-modified PGE show a good electrocatalytic oxidation towards L-dopa (as seen in Fig. 3A), indicating that the CNT-modified PGE can effectively decrease the oxidation potential of L-dopa to 0.196 V. However, a pair of well-defined redox peaks is observed at the AuNP-CNT/PGE. The anodic and cathodic peak potentials are at 0.212 and 0.173 V, respectively, with a peak-to-peak separation of about 0.039 V. Furthermore, the oxidation peak current ( $I_{pa}$ ) of L-dopa at the AuNP-CNT/PGE is 28.3- and 1.67-fold higher than that of the bare and CNT-modified PG electrodes, with a better reversibility. These results confirm that the Au nanoparticles on CNT surface can effectively accelerate the electrochemical redox of L-dopa and significantly increase the oxidation current at the modified electrode.

The relationship between redox peaks current is also investigated with CV method. The anodic and cathodic currents are linear with the square root of the scan rate from 20 to 200  $\text{mV s}^{-1}$ . The linear progress equation are  $I_{pa}(10^{-6} \text{ A}) = (2.905 \pm 1.112) + (0.307 \pm 0.009)\nu$  and  $I_{pc}(10^{-6} \text{ A}) = (10.370 \pm 1.206) - (0.285 \pm 0.009)\nu$  ( $\text{mV s}^{-1}$ ), a correlation coefficient of 0.997 and 0.996, respectively, indicating that the electrode progress is controlled by adsorption [38]. The most probable reason is that the electronegative oxygen-containing groups and gold nanoparticles on CNTs surface can easily adsorb electropositive L-dopa molecule in neutral PBS blank.

#### 3.3. Effects of solution pH

Cyclic voltammetry was carried out to characterize the effects of solution pH on redox peak potentials of L-dopa at the AuNP-CNTs/PGE in Fig. 4. As shown in Fig. 4A, the redox peak potential of L-dopa shifts negatively with the increase of solution pH, indicating that protons take part in the electrode reaction process. The anodic peak potential of L-dopa is proportional with the solution pH in the range of 3–10. The linear regression equation was  $E_{pa}(\text{V}) = (0.606 \pm 0.014) - (0.057 \pm 0.001)\text{pH}$ , with the correlation coefficient 0.999, demonstrating that the electrode process is equal proton-electron transfer. The slope of the equation is in close agreement with the former report [27]. For a reversible electrochemical

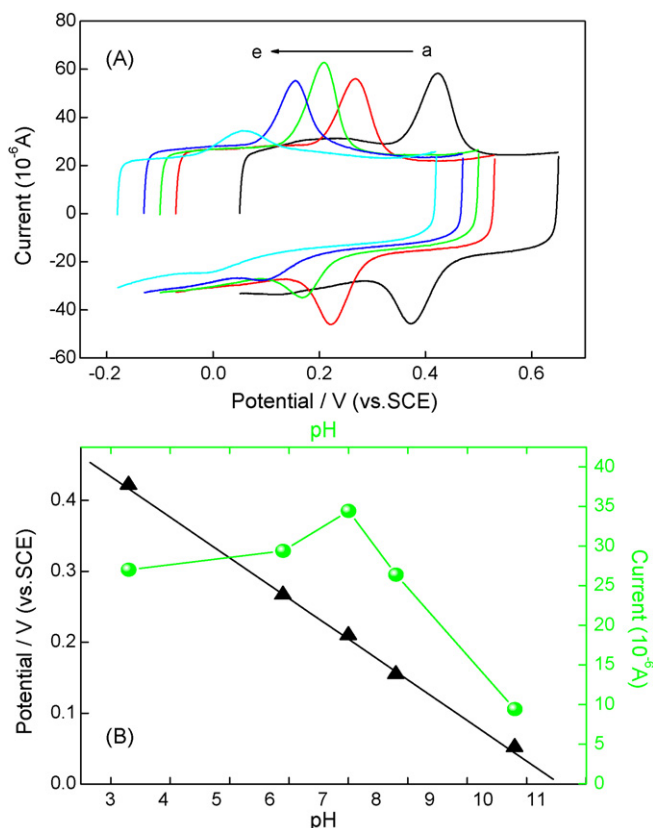
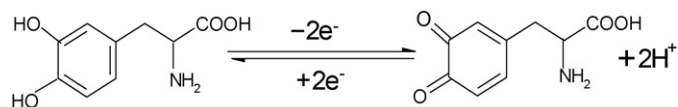


Fig. 4. (A) CV curves of CNT/PGE in 0.1 M PBS containing 20  $\mu\text{M}$  L-dopa at different pH: a  $\rightarrow$  e, 3.3, 5.9, 7.0, 7.8, and 9.8; (B) dependence of anodic peak potential (black triangle) and anodic peak current (green globular) as a function of solution pH in 0.1 M PBS containing 20  $\mu\text{M}$  L-dopa. (For interpretation of the references to color in this figure legend, the reader is referred to the web version of the article.)

reaction,  $|E_p - E_{p/2}| = 59/n \text{ mV}$ , the electron transfer number was calculated to be 1.843 (approximately 2). So the electrochemical redox of L-dopa at the proposed electrode is a two-electron coupled two-proton transfer mechanism. Therefore, the electrochemical redox process of L-dopa can be described as follows:



#### 3.4. Effect of accumulation time

As the electrode progress is controlled by the adsorption of L-dopa, it is very important to investigate the effects of accumulation time. As shown in Fig. 5, the oxidation peak current of L-dopa gradually increased with increasing accumulation time from 0 to 180 s, and reached the maximum current response at 180 s. Further increasing the accumulation time, there is no significant increase in the current response. This phenomenon is probably due to the saturated adsorption of L-dopa on the AuNP-CNT/PGE surface, and no change is observed when increasing the accumulation time. Herein, 180 s is chosen as the optimum accumulation time. The accumulation potential was also investigated in the range of  $-0.4$  to  $0.1$  V. The results prove that varying accumulation potential does not show sufficient influence on the increase of L-dopa oxidation current. Therefore, a stirred accumulation for 180 s under open-circuit was used for the preconcentration of L-dopa in each voltammetric measurement.

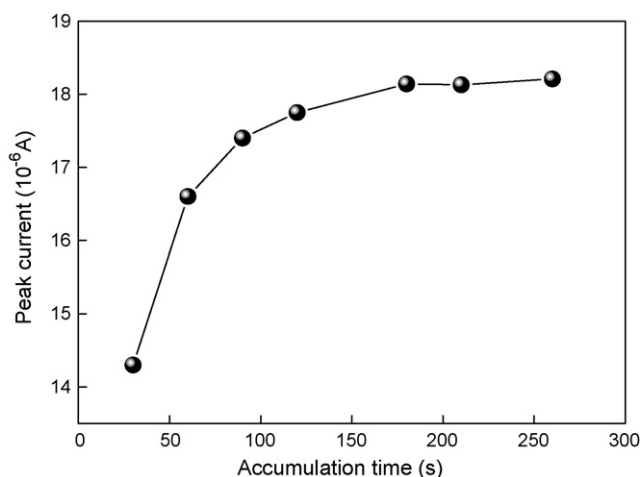


Fig. 5. Effect of accumulation time on peak current of 10  $\mu\text{M}$  L-dopa at AuNP-CNT/PGE in 0.1 M PBS at pH 7.0.

### 3.5. DPV determination of L-dopa

Differential pulse voltammetry (DPV) method is normally used for the determination of catecholamine compounds because of its high sensitivity [39,40]. Herein, the determination of L-dopa was also performed with the DPV method using the proposed AuNP-CNT/PGE. Fig. 6 shows the DPV curves at different concentrations of L-dopa at the modified electrode. Clearly, the anodic peak current increases linearly with L-dopa concentration ranging from 0.1 to 150  $\mu\text{M}$ , the linear regression is  $I_{\text{p-L-dopa}} (\mu\text{A}) = (0.388 \pm 0.596) + (1.073 \pm 0.011) (\mu\text{M})$ , with a correlation coefficient of 0.998. The detection limit is 50 nM ( $S/N = 3$ ), which is better than that of the latest reports [30,41,42]. The relative standard deviation of 10 determinations for 10  $\mu\text{M}$  is 0.93%, showing the good reproducibility of the proposed electrode. The anodic current of L-dopa has no significant change at the proposed electrode after its preparation for 2 months, indicating the excellent stability of Au-CNT/PGE.

### 3.6. Interference study

It is well known that UA and AA are electroactive molecules that coexist in a biological system [43], and that they can also be oxidized in most conventional solid electrodes. Therefore, it is

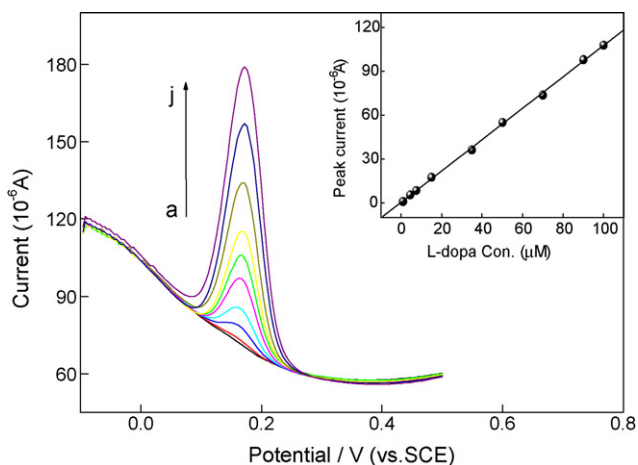


Fig. 6. DPV curves of Au-CNT/PGE in 0.1 M PBS (pH 7.0) containing different concentration L-dopa: a  $\rightarrow$  j, 0, 1, 4.5, 7.5, 15, 35, 50, 70, 90, and 100  $\mu\text{M}$ . Inset is the linear relationship between  $I_{\text{pa}}$  and L-dopa concentration.

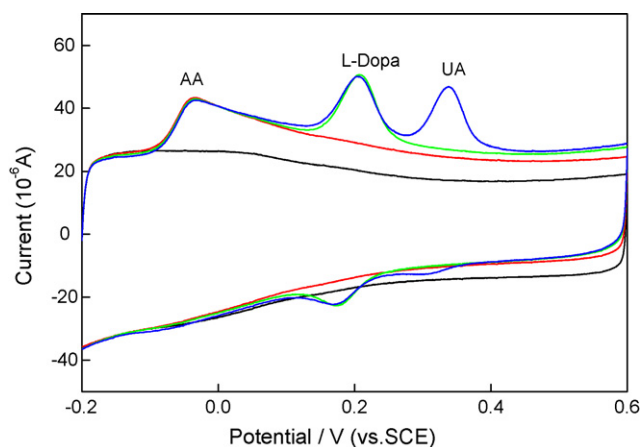


Fig. 7. CV curves of the Au-CNT/PGE (black line) by successively adding 1.0 mM AA (red line), 20  $\mu\text{M}$  L-dopa (green line) and 20  $\mu\text{M}$  UA (blue line) in 0.1 M PBS at pH 7.0. (For interpretation of the references to color in this figure legend, the reader is referred to the web version of the article.)

Table 1

Determination of L-dopa in capsules ( $n = 5$ ).

| Sample No. | Labeled (mg) | Detected (mg) | RSD   | Recovery | Bias (%) |
|------------|--------------|---------------|-------|----------|----------|
| 1          | 200          | 196 $\pm$ 3   | 1.53% | 98%      | -2.0     |
| 2          | 200          | 206 $\pm$ 5   | 1.84% | 103%     | +3.0     |
| 3          | 200          | 203 $\pm$ 4   | 1.74% | 102%     | +1.5     |

important to investigate these interferences in order to conduct the accurate determination of L-dopa. Fig. 7 shows three individual anodic peaks appearing at the potential of -0.037, 0.208 and 0.336 V, which correspond to the oxidations of AA, L-dopa and UA, respectively. The results illustrate that the coexistence of UA and AA has no influence on L-dopa determination. Equivalent amount of dopamine and epinephrine will seriously affect the accurate determination of L-dopa. As their concentration in human blood and urine is extremely low, so dopamine and epinephrine do not affect the determination of L-dopa in human fluids. The influence of other substances on L-dopa peak currents was also investigated, and no interference was found for 10  $\mu\text{M}$  L-dopa in the presence of the following substances: 100-fold glucose, urea and 1000-fold  $\text{NO}_3^-$ ,  $\text{Cl}^-$ ,  $\text{PO}_4^{3-}$ ,  $\text{SO}_4^{2-}$ ,  $\text{NH}_4^+$ ,  $\text{K}^+$ ,  $\text{Na}^+$ ,  $\text{Mg}^{2+}$ ,  $\text{Ca}^{2+}$ , with a deviation below 5%.

### 3.7. Sample analysis

In order to evaluate the validity of the proposed method, contents of 30 hard capsules were emptied, weighed and carefully mixed. A portion of the powder equivalent to 500 mg L-dopa was accurately weighed, dissolved into 10 mL of 0.1 M  $\text{H}_2\text{SO}_4$  and separated with a centrifugal machine. Further dilution was also performed with 0.1 M  $\text{H}_2\text{SO}_4$  to reach the calibration range of L-dopa. A standard addition was used for L-dopa concentration determination in 0.1 M PBS at pH 7.0. The recoveries were 98–103%, with a relative standard deviation (RSD) lower than 2% (in Table 1), confirming that the proposed sensor is reliable for L-dopa determination in pharmaceutical preparations.

## 4. Conclusions

High-quality gold nanoparticle-functionalized carbon nanotube material has been successfully synthesized via self-assembly technology. The new material can be considered as a high sensitive and selective sensor in voltammetric determination of L-dopa. The proposed sensor shows a novel electrocatalytic activity towards the

anodic oxidation of L-dopa with a significant enlargement in peak current and a great decrease in peak potential. The reproducibility, good selectivity and stability, low detection limit of the proposed electrode make it appropriate for use in the electrochemical determination of L-dopa in pharmaceutical and clinical preparations.

### Acknowledgements

The authors thank the financial support of National Natural Science Foundation of China (No. 20672121) and the open fund of State Key Laboratory of Oxo Synthesis & Selective Oxidation (Grant No. OSSO2008kjk6).

### References

- [1] J. Hardy, K. Gwinn-Hardy, *Science* 282 (1998) 1075–1079.
- [2] Schapira A.H.V., *J. Neurol. Neurosurg. Psychiatry* 76 (2005) 1472–1478.
- [3] E.R. Ritvo, A. Yuwiler, E. Geller, A. Kales, S. Rashkis, A. Schicor, S. Plotkin, R. Axelrod, C. Howard, *J. Autism Childhood Schizophrenia* 1 (1971) 190–205.
- [4] A. Barbeau, *Adv. Neurol.* 5 (1974) 347–365.
- [5] L.V. Laitinen, A.T. Bergenheim, M.I. Hariz, *J. Neurosurg.* 76 (1992) 53–61.
- [6] E.J. Greenhow, L.E. Spencer, *Analyst* 98 (1973) 485–492.
- [7] B.A. Hasan, K.D. Khalaf, M.D.L. Guardia, *Talanta* 42 (1995) 627–633.
- [8] P. Siddhuraju, K. Becker, *Food Chem.* 72 (2001) 389–394.
- [9] S. Thiagarajan, S.-M. Chen, *Talanta* 74 (2007) 212–222.
- [10] R.J. Mascarenhas, K.V. Reddy, B.E. Kumaraswamy, B.S. Sherigara, V. Lakshminarayanan, *Bull. Electrochem.* 21 (2005) 341–345.
- [11] M.F.S. Teixeira, M.F. Bergamini, C.M.P. Marques, N. Bocchi, *Talanta* 63 (2004) 1083–1088.
- [12] M.F. Bergamini, A.L. Santos, N.R. Stradiotto, M.V.B. Zanoni, *J. Pharm. Biomed. Anal.* 39 (2005) 54–59.
- [13] A. Sivanesan, S.A. John, *Biosens. Bioelectron.* 23 (2007) 708–713.
- [14] J. Di, C. Shen, S. Peng, Y. Tu, S. Li, *Anal. Chim. Acta* 553 (2005) 196–200.
- [15] S. Lü, *Microchem. J.* 77 (2004) 37–42.
- [16] M.E.B. Calvo, O.D. Renedo, M.J.A. Martínez, *Talanta* 74 (2007) 59–64.
- [17] A. Salimi, A. Noorbakhash, E. Sharifi, A. Semnani, *Biosens. Bioelectron.* 24 (2008) 792–798.
- [18] S.A. Kumar, H.W. Cheng, S.M. Chen, S.F. Wang, *Mater. Sci. Eng. C* 30 (2010) 86–91.
- [19] R.N. Goyal, V.K. Gupta, S. Chatterjee, *Biosens. Bioelectron.* 24 (2009) 1649–1654.
- [20] R.N. Goyal, V.K. Gupta, S. Chatterjee, *Biosens. Bioelectron.* 24 (2009) 3562–3568.
- [21] R.N. Goyal, V.K. Gupta, S. Chatterjee, *Electrochim. Acta* 53 (2008) 5354–5360.
- [22] R.N. Goyal, V.K. Gupta, M. Oyama, N. Bachheti, *Talanta* 71 (2007) 1110–1117.
- [23] R.N. Goyal, V.K. Gupta, M. Oyama, N. Bachheti, *Electrochem. Commun.* 7 (2005) 803–807.
- [24] R.N. Goyal, V.K. Gupta, A. Sangal, N. Bachheti, *Electroanalysis* 17 (2005) 2217–2223.
- [25] R.N. Goyal, V.K. Gupta, N. Bachheti, R.A. Sharma, *Electroanalysis* 20 (2008) 757–764.
- [26] R.N. Goyal, V.K. Gupta, S. Chatterjee, *Talanta* 76 (2008) 662–668.
- [27] X. Yan, D. Pang, Z. Lu, J. Lu, H. Tong, *Electroanal. Chem.* 569 (2004) 47–52.
- [28] C. Xiang, Y. Zou, J. Xie, X. Fei, *Anal. Lett.* 39 (2006) 2569–2579.
- [29] J. Mathiyarasu, L. Nyholm, *Electroanalysis* 22 (2010) 449–454.
- [30] S. Shahrokhian, E. Asadian, *Electroanal. Chem.* 636 (2009) 40–46.
- [31] G. Hu, Y. Guo, S. Shao, *Electroanalysis* 21 (2009) 1200–1206.
- [32] L. Zhang, X. Jiang, *Electroanal. Chem.* 583 (2005) 292–299.
- [33] R.N. Goyal, V.K. Gupta, M. Oyama, N. Bachheti, *Talanta* 72 (2007) 976–983.
- [34] L. Chen, H. Liu, K. Yang, J. Wang, X. Wang, *Mater. Chem. Phys.* 112 (2008) 407–411.
- [35] S. Xu, Q. Yang, *J. Phys. Chem. C* 112 (2008) 13419–13425.
- [36] L. Chen, G. Hu, G. Zou, S. Shao, X. Wang, *Electrochem. Commun.* 11 (2009) 504–507.
- [37] A.L. Rogach, A. Kornowski, M. Gao, A. Eychmüller, H. Weller, *J. Phys. Chem. B* 103 (1999) 3065–3069.
- [38] A.J. Bard, L.R. Faulkner, *Electrochemical Methods: Fundamentals and Application*, Wiley, New York, 1980, pp. 218–220.
- [39] S. Zhu, H. Li, W. Niu, G. Xu, *Biosens. Bioelectron.* 25 (2009) 940–943.
- [40] H.R. Zare, N. Nasirizadeh, M.M. Ardakani, *Electroanal. Chem.* 577 (2005) 25–33.
- [41] M. Aslanoglu, A. Kutluay, S. Goktas, S. Karabulut, *J. Chem. Sci.* 121 (2009) 209–215.
- [42] M.F.S. Teixeira, L.H. Marcolino-Júnior, O. Fatibello-Filho, E.R. Dockal, M.F. Bergamini, *Sens. Actuators B* 122 (2007) 549–555.
- [43] P. Fossati, L. Prencipe, G. Berti, *Clin. Chem.* 26 (1980) 227–231.